Array size scaling of passive coherent beam combination in fiber laser array

Yuhao Xue (薛宇豪)[1,2,3], Bing He (何 兵)[1,2*], Jun Zhou (周 军)[1,2], Jinchong Xue (薛晋冲)[4], Zhen Li (李 震)[1,2,3], Houkang Liu (刘厚康)[1,2,3], and Qihong Lou (楼祺洪)[1,2]**

[1]*Research Center of Space Laser, Shanghai Institute of Optics and Fine Mechanics, Chinese Academy of Sciences, Shanghai 201800, China*

[2]*Shanghai Key Laboratory of All Solid-State Laser and Applied Techniques, Shanghai 201800, China*

[3]*Graduate University of Chinese Academy of Sciences, Beijing 100049, China*

[4]*PLA'S Artillery Command Academy, Zhangjiakou 075100, China*

[*]*Corresponding author: bryanho@siom.ac.cn;* [**]*corresponding author: junzhousd@siom.ac.cn*

Received March 24, 2011; accepted June 10, 2011; posted online August 24, 2011

Array size scaling of passive coherent beam combination is explored theoretically. The Strehl ratio variation with wavelength is simulated in 4-, 9-, 16-, and 25-channel fiber arrays. The average Strehl ratio and phase error are calculated. The Strehl ratio is found to be near 100% for arrays with less than 5 fibers, but decreases significantly for larger arrays. These results are in good agreement with the recent experimental results.

OCIS codes: 140.3510, 140.3298, 140.3290.
doi: 10.3788/COL201210.011401.

Coherent beam combination (CBC) of a fiber laser array can achieve power scaling while maintaining near diffraction limited (DL) performance. Numerous techniques have been proposed and demonstrated. CBC can be classified into two categories, namely, active phasing[1−4] and passive phasing[5−13]. Active phasing requires complicated phase detection and phase modulation for each element of the array. Locking the phase stably is difficult when the number of combining elements is large. Passive phasing is realized by the self-adjusting process of the resonance frequencies of fiber laser arrays to adapt to changes in the optical path lengths. Passively phase-locked techniques have been reported including self-Fourier laser cavity[5,6], self-imaging resonator[7−9], all-fiber combining[10], self-organization mechanism in fiber laser arrays[11,12], and mutual injection locking lasers[13]. However, most of the reports have focused on power boost and phase noise and the characteristic of array size scaling is taken into account rarely in CBC. Array size scaling is one of the important factors for power scaling in CBC. Array size scaling of passive beam phasing can be estimated using the Strehl ratio, combining efficiency, and beam quality. The Strehl ratio represents far-field peak intensity. Combining efficiency is the ratio between the output powers of phase locking and non-locking. Beam quality shows energy concentration in the far field.

In this letter, we conduct theoretical study on the passive CBC of multi-channel fiber laser arrays based on a typical ring cavity. The Strehl ratio variation with wavelength is simulated in 4-, 9-, 16-, and 25-channel fiber arrays. The average Strehl ratio and phase error variation in relation to the number of fibers are calculated. When the array size increases, the average Strehl ratio decreases significantly while phase error increases. These results are compared with recent experiments and in good agreement with the recent expermental results.

As a model system for studying passive CBC, a configuration of fiber amplifier array with a ring cavity is chosen. The configuration has been demonstrated in an earlier phase locking experiment[15]. The model system, shown in Fig. 1, consists of N fiber amplifiers (A) and single mode feedback fiber (FF) loop. At the output end of the fiber amplifiers, collimators (Co) transform the output beams into a compact array of parallel beams. The major part of the beam power is output through a beam splitter (BS). The rest weak fraction of power is reflected by the beam splitter and coupled into the single mode FF that provides the seed for all the amplifiers. The FF is located at the focus of lens (L) as a filter.

In this system, the longitudinal modes with high peak intensity are coupled into the FF loop, and other longitudinal modes are suppressed. The Strehl ratio can show peak intensity in the far field. Thus, it can be used to represent the transmission efficiency of the filter. The optical path length of each fiber amplifier ranges from several meters to tens of meters. Ensuring equal lengths

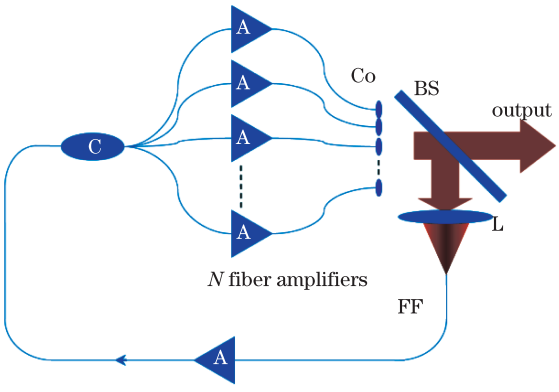

Fig. 1. Architecture of a passive coherent beam combination with a ring cavity.

is practically impossible. In addition, the optical path lengths are constantly changing due to thermal and mechanical effects, and thus, their phases randomly change. The typical roundtrip time for a fiber channel is in the order of hundreds of nanoseconds, and the frequency of optical path length variation is from hundreds to thousands of hertzs. Therefore, the optical path length of each channel can be seen as a constant in a short time (Δt= 1 ms). The phase of every amplifier output is written as

$$\phi_i = 2\pi f(nL)_i/c, \tag{1}$$

where f is the longitudinal mode frequency and $(nL)_i$ is the optical path length of the ith fiber channel. Given that the average value of the fiber optical path lengths is $(nL)_{\rm avg}$, the relative phase of fiber output is given by

$$\phi_i' = 2\pi f[(nL)_i - (nL)_{\rm avg}]/c. \tag{2}$$

Assuming all fiber outputs have fields that are equal with unity amplitudes, the Strehl ratio of the combined beam in FF can be written as

$$S = \Big|\sum_{i=1}^{N} \exp(\mathrm{i}\phi_i')\Big|/N^2 = \Big|\sum_{i=1}^{N} \exp\{\mathrm{i}2\pi f[(nL)_i - (nL)_{\rm avg}]/c\}\Big|/N^2. \tag{3}$$

At this point, we consider the case of a large number of fiber channels, where the fiber lengths are normally distributed with several root mean square (RMS) variations, $(nL)_{\rm RMS}$. An earlier study[16] has shown that the Strehl ratio variation with frequency bandwidth can be represented by a Gaussian function as

$$S(f - f_0) = \exp[-4\pi^2 (f - f_0)^2 (nL)_{\rm RMS}^2/c^2]. \tag{4}$$

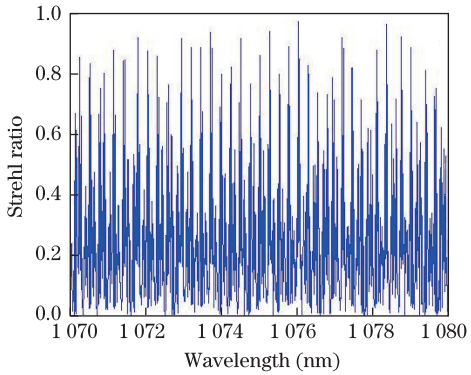

Fig. 2. Strehl ratio versus wavelength in a 4-channel fiber array.

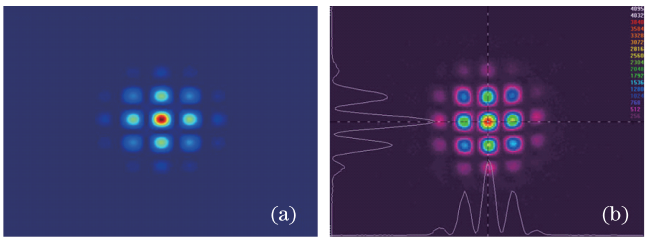

Fig. 3. (a) Calculated and (b) experimental beam profiles in the far field for four-channel fiber array.

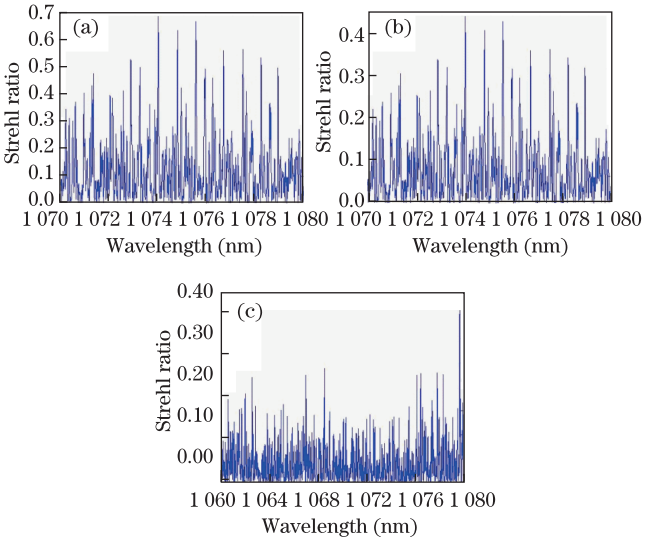

Fig. 4. Strehl ratio versus wavelength in an N-channel fiber array. (a) N=9, (b) N=16, and (c) N=25.

Nabors has demonstrated that the phase error can be obtained using the Strehl ratio as[17]

$$\sigma = \sqrt{\ln \frac{N-1}{NS-1}}. \tag{5}$$

Firstly, a 4-channel fiber array is simulated according to Eq. (4). The optical path lengths of the channels are assumed to be 20.941, 21.020, 21.011, and 21.052 m. Figure 2 shows a simulation of the Strehl ratio variation with wavelength. Numerous longitudinal modes with high Strehl ratios of over 0.8 are found. When the wavelength is 1 076.0294 nm, the relative phases are $0.0213\times2\pi$, $0.0897\times2\pi$, $0.0059\times2\pi$, and $0.0540\times2\pi$. The maximum phase error is $0.0838\times2\pi$, and the Strehl ratio is 0.97. According to Ref. [17], the beam profile in the far field is simulated with a wavelength of 1 076.0294 nm. Figure 3 shows the calculated and experimental beam profiles in the far field when the near-field beam of fiber array is arranged for the square.

Furthermore, the Strehl ratio variation with wavelength is simulated in 9-, 16-, and 25-channel fiber arrays, as shown in Fig. 4. The average value $(nL)_{\rm avg}$ of fiber optical path lengths is 21 m, and the variation of these optical path lengths is 1-cm RMS. The maximum Strehl ratio is 0.36 for 25 channels, and only a few longitudinal modes with a Strehl ratio of over 0.2 exist, as shown in Fig. 4(c). Because of the increase in channel number, the maximum Strehl ratio decreases and the number of longitudinal modes with a high Strehl ratio decreases as well. Figure 5 shows the calculated beam profiles in the far field for 9-, 16-, and 25-channel fibers array when the near-field beam of fiber arrays is arranged for the square.

To describe the relationship between the Strehl ratio and array size better, the maximum Strehl ratios are determined for each realization in the ensemble and subsequently averaged to find the expected Strehl performance for a given fiber array. Figure 6 shows the average Strehl ratio and phase error variation with the number of fibers. The calculated Strehl ratio is

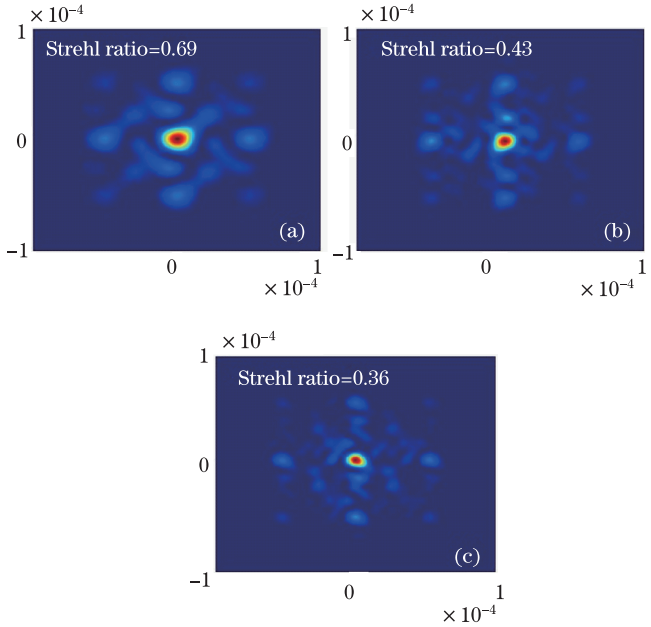

Fig. 5. Calculated beam profiles in the far field for an N-channel fiber array. (a) N=9, (b) N=16, and (c) N=25.

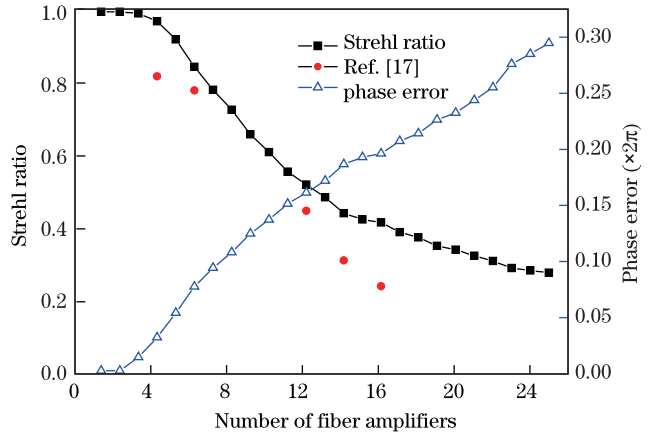

Fig. 6. Average Strehl ratio and phase error variation in relation to the number of fibers.

nearly 100% for arrays with less than 5 fibers, but decreases significantly for larger arrays. The dot in Fig. 6 is the approximation of experimental results of Ref. [18]. The theoretical results are in good agreement with the experimental results.

In conclusion, theoretical analysis and numerical simulations are presented for passive CBCs of 4-, 9-, 16-, and 25-channel fiber arrays. The maximum Strehl ratio decreases and the number of longitudinal modes with a high Strehl ratio decreases with the increase in array size. The Strehl ratio is nearly 100% for arrays with less than 5 fibers, but decreases significantly for larger arrays. These results are in good agreement with recent experiments.

This work was supported by the National Natural Science Foundation of China (No. 60908011), the National High Technology Research and Development Program of China (No. 2011AA030201), the Shanghai "Phosphor" Science Foundation, China (No. 09QB1401700), and the National Science and Technology Major Project (No. 2010ZX04013).

References

1. J. Anderegg, S. Brosnan, E. Cheung, P. Epp, D. Hammons, H. Komine, M. Weber, and M. Wickham, Proc. SPIE **6102,** 1 (2006).
2. P. Zhou, Z. Liu, X. Wang, Y. Ma, H. Ma, and X. Xu, Appl. Phys. Lett. **94,** 231106 (2009).
3. E. C. Cheung, J. G. Ho, G. D. Goodno, R. R. Rice, J. Rothenberg, P. Thielen, M. Weber, and M. Wichham, Opt. Lett. **33,** 354 (2008).
4. X. Fan, J. Liu, J. Liu, and J. Wu, Chin. Opt. Lett. **8,** 48 (2010).
5. C. J. Corcoran and K. A. Pash, J. Opt. A **7,** L1 (2005).
6. C. J. Corcoran and F. Durville, Appl. Phys. Lett. **86,** 201118 (2005).
7. B. He, Q. Lou, J. Zhou, J. Dong, Y. Wei, D. Xue, Y. Qi, Z. Su, L. Li, and F. Zhang, Opt. Express **14,** 2721 (2006).
8. W. Wang, B. He, H. Zhang, Y. Xue, Z. Li, X. Liu, J. Zhou, and Q. Lou, Chin. Opt. Lett. **8,** 680 (2010).
9. W. Wang, Q. Lou, B. He, J. Zhou, Z. Li, Y. Xue, and X. Liu, Chin. Opt. Lett. **8,** 490 (2010).
10. B. Wang, E. Mies, M. Minden, and A. Sanchez, Opt. Lett. **34,** 863 (2009).
11. E. J. Bochove, P. K. cheo, and G. G. King, Opt. Lett. **28,** 1200 (2003).
12. H. Bruesselbach, D. Cris Jones, M. Mangir, M. Minden, and J. Rogers, Opt. Lett. **30,** 1339 (2005).
13. S. Auroux, V. Kermène, A. Desfarges-Berthelemot, and A. Barthélémy, Opt. Express **17,** 17694 (2009).
14. J. Lhermite, A. Desfarges-Berthelemot, V. Kermene, and A. Barthelemy, Opt. Lett. **32,** 1842 (2007).
15. W. Chang, T. Wu, H. Winful, and A. Galvanauskas, Opt. Express **18,** 9634 (2010).
16. J. Rothenberg, Proc. SPIE **6873,** 687315 (2008).
17. C. D. Nabors, Appl. Opt. **33,** 2284 (1994).
18. S. Shakir, B. Culver, B. Nelson, Y. Starcher, Proc. SPIE **7070,** 70700N (2008).